SCIENCE CHINA
Technological Sciences

• Article •

August 2015 Vol.58 No.8: 1414–1424
doi: 10.1007/s11431-015-5838-8

Experimental and numerical investigations on dynamic and acoustic responses of a thermal post-buckled plate

GENG Qian, WANG Di, LIU Yuan & LI YueMing*

State Key Laboratory for Strength and Vibration of Mechanical Structures, Xi'an Jiaotong University, Xi'an 710049, China

Received December 28, 2014; accepted April 8, 2015; published online June 10, 2015

Experiments were carried out for a clamped rectangular aluminum plate to study the dynamic and acoustic behaviors in both pre- and post-buckling ranges under thermal loads. Plate temperature was elevated from ambient value to the level above the theoretical critical buckling temperature of the plate. In the whole test temperature range, the measured frequencies decreased to the minimum values in sequence, and then turned to increase as temperature rose. The softening effect of thermal stresses played the leading role in the decreasing stage and the stiffening effect of thermal buckling deflection became the major influence factor in the increasing stage. The later one could drive the temperature equilibrium point of the heated plate to move towards lower temperature range. All the frequencies would not drop to zero due to the inherent initial deflection which provides additional stiffness to the plate. Dynamic responses state two variation trends in different temperature ranges, shifting toward the lower frequency range and closing up in the mid-frequency range. The characters of spectrum responses changed gradually as the temperature was elevated. Numerical simulations gave predictions with same variation trend as the test results.

thermal post-buckled plate, modal test, dynamic response test, numerical simulation

Citation: Geng Q, Wang D, Liu Y, et al. Experimental and numerical investigations on dynamic and acoustic responses of a thermal post-buckled plate. Sci China Tech Sci, 2015, 58: 1414–1424, doi: 10.1007/s11431-015-5838-8

1 Introduction

Thermal environment is an important influence factor for various engineering structures, such as spacecraft, vehicle engine, and so on. Temperature variations may change the material properties, the stress state and the configuration of structures, and will influence the static and dynamic performance during working [1,2]. In the meanwhile, structures also work under sorts of loads and excitations along with thermal variations [3–6]. The service environment is usually highly integrated and complicated.

Responses of complex structures in combined environment have been analyzed with numerical simulations [7,8] to predict the behaviors under different factors. Studies of typical structures have also been carried out numerically and analytically to reveal the mechanism. Jeyaraj et al. [9,10] used the combined approach of finite element and boundary element method (FEM/BEM) to study the vibration and acoustic responses of isotropic and composite plates in thermal environments. Thermal effects were considered via prestress analyses. Geng and Li [11,12] investigated the influence of thermal stresses on simply supported and fully clamped plates with theoretical and numerical analyses. Responses were obtained based on the governing equation of plates with thermally induced membrane forces. Liu and Li [13] studied the response characters of rectangular sandwich plates with temperature variations. Equivalent non-classical theory with the shear and rotational inertia was used in the work. Li and Li [14] employed the first-order shear deformation theory to study the response characters of the laminated plates in thermal environments. Results

*Corresponding author (email: liyueming@mail.xjtu.edu.cn)

from the above literature show decrements of natural frequencies for the heated plates. Response curves shift toward the lower frequency range, and the radiation efficiency varies oppositely in frequency ranges below and above the critical frequency.

Experimental work has also been done on this topic. For real structures, McWithey and Vosteen [15] conducted experimental researches on the fundamental mode of an X-15 prototype wing under uniform and non-uniform heating. Brown [16] carried out experimental investigations on the modal characters of X-34 FASTRAC composite rocket nozzle at high temperature. FEM programs were also coded to study the test results. Modal tests were also carried out with X-37 ruddervator subcomponent in thermal environments [17,18]. Results indicate that thermal stresses will affect structural stiffness significantly. Wu et al. [19] conducted modal tests of a hollow wing structure in high thermal environments. They found that the natural frequencies of the wing kept decreasing in the whole test temperature range. For elementary structures, Vosteen and Fuller [20] designed a set of test facilities for the heated cantilever plates and measured the low order natural vibrations. Result implies that natural frequencies of the first bending mode and the first torsion mode reduce with the increment of temperature. Plates with solid double-wedge and circular-arc multiweb-wing sections were also tested [21]. Kehoe and Snyder [22,23] carried out modal tests for aluminum plates with free boundaries under thermal loads. Numerical simulations were performed to investigate the problem as well. A decrement of natural frequencies and an increment of damping capacity were detected when the plate was heated. Kehoe and Deaton [24] provided experimental researches on modal characters of plates under steady and transient heating. They found that the material property variations and thermal stresses were the primary reasons for the reduction of structural stiffness. Amabili and Carra [25] employed experimental and numerical methods to study the nonlinear forced vibration of thermal loaded plates, and found that geometric imperfection could affect the nonlinear responses obviously. Joen et al. [26] carried out researches on natural vibrations of rectangular aluminum plates with free boundaries under different heating rates. Some mode shapes disappeared when structural temperature rose. It is clear from the literature that experimental work was conducted almost for hot structures with free boundaries. However, the response characteristics greatly depend on the boundary condition in thermal environments. Geng et al. [27] performed experimental researches on dynamic and acoustic response of a heated clamped plate. Decrement of natural frequencies was observed in modal tests, and the dynamic responses of the plate shifted toward lower frequency range. Numerical simulations imply that the initial deflection influences the behavior of the clamped plate in thermal environments.

For constrained structures, buckling will occur when temperature rises above the critical value [28,29]. The equilibrium state of the heated structure will be changed, and this will affect the dynamic responses of the heated structures. For the buckled structures, Tawfik et al. [30] analyzed the fundamental frequency of the thermal buckled shape memory alloy plates with finite element method. Singha et al. [31] studied the dynamic characters of the thermal post-buckled composite plates with high precision plate bending elements. Xia and Shen [32,33] developed the theoretical formulation for the dynamic response of the thermal post-buckled functionally graded material plate, and analyzed the variation in frequencies with temperature changes. Fazzolari and Carrera [34] studied the free vibration response of pre- and post-buckled anisotropic multilayered plates with considering coupled thermo-mechanical effect. The above researches were based on theoretical and numerical methods. Results indicate that the fundamental frequency decreases to zero at the critical buckling point, and turns to increase in higher temperature range. Murphy et al. [35,36] predicted the natural frequencies of the clamped plate in thermal environment theoretically. Good agreements were obtained with experimental results. As described above, it reveals that few experimental studies have been carried out to investigate the response characters of thermal buckled plates. And the existing work just focused on the natural vibrations of thermal loaded structures. The forced vibration and acoustic radiation responses are seldom considered.

The present work performed experimental and numerical investigations of a fully clamped rectangular plate in pre- and post-buckling ranges under thermal loads. Modal tests and forced vibration response tests were carried out with thermal variations in the temperature range below and above the theoretical critical buckling temperature of the plate. Numerical simulations were employed to study the phenomena observed in the tests, and comparisons were made between the idealized flat plates and real plates.

2 Test methodology

2.1 Experimental setup

The test system was the same as used in ref. [27]. The specimen, a rectangular plate, was placed horizontally on the top of the supporting foundations. The heating equipment, four quartz lamps, was set below the test plate, and measuring devices were arranged on the other side. Heat flux generated from the lamps was controlled by a voltage regulator to change the plate temperature and keep it constant during each test. Thermal insulation blanket material was attached on the inside wall of the experimental frames. The schematic of the test setup is shown in Figure 1.

The dimensions of the specimen were 0.4 m×0.3 m×0.003 m with an area of 0.3 m×0.2 m in the center for testing. The test region was equally divided into 50 blocks by nine and four split lines along the length and width of the

plate, respectively. Thirty six test points were marked on the intersections of the lines. The plate was fastened to the foundations with 24 bolts on four edge margins with the width of 0.05 m. Material properties of the specimen were Young's modulus 65 GPa, Poisson's ratio 0.27, mass density 2810 kg m^{-3}, and thermal expansion coefficient 2.3×10^{-5} K^{-1}. The elastic parameters were determined via impact modal tests at room temperature during preliminary work.

2.2 Test procedures

Firstly, modal tests were carried out to study the influence of thermal variations on natural vibration of the clamped plate. The test procedure was implemented via single-input single-output hammer based impact method (PCB hammer 086C04). An accelerometer (PCB 333B32) was located on a proper location to acquire the impact responses of the plate with avoiding nodal lines of low order modes. The plate was impacted on all the 36 points in sequence to obtain the mode shapes. Each point was excited repeatedly, and five spectral responses with good coherence were finally selected. Coherence checks were implemented in the test system during each impact. Responses were acquired within one second after excitations in the bandwidth of 2560 Hz with a resolution of 0.625 Hz. The Impact Testing module of the software package LMS TEST.LAB was used for signal acquisitions and data analyses.

Dynamic response measurements were made under acoustic and mechanical excitations, respectively. As described in Figure 1(a) [27], the acoustic source was generated by a loudspeaker (Alpine SPS-170A) installed 0.3 m above the plate center, and applied through a power amplifier (B&K type 2718). Vibration responses of the plate on some observation points were acquired by accelerometers (PCB 333B32). The test system for mechanical excitations used in the present work was modified from the previous one [27], due to higher test temperature. As depicted in Figure 1(b), the exciter (MB Exciter Modal 2) was hung over the specimen and connected to the plate with a rod to apply the excitations. The excitation signals were acquired with a force transducer (Lance LC2301) connected to the exciter as the reference signals. Acceleration responses on the plate were detected, and the radiated sound pressures were acquired with a microphone (B&K type 4961) set 0.4 m vertically above the plate. In preliminary tests, it had been confirmed that the level of the noise generated from the working exciter is much lower than the sound radiated from the specimen. The disturbance of the exciter on the test results could be neglected. Accelerometers and the force transducer were fixed on the plate with bakelite bricks to keep the sensors working under the permitted temperature.

As the spectral responses under periodic chirp signals can be obtained more rapidly than single-frequency signals, the responses are much clearer than other frequency-swept signals provided in the test system, such as random or burst signals. Periodic chirp signals were selected as the excitation form in the tests. This had been confirmed in preliminary tests. Responses were all detected in the bandwidth of 4096 Hz with a resolution of 0.5 Hz. Dynamic tests were implemented by the Spectral Testing module of the software package LMS TEST.LAB to achieve the excitation control and data processing.

2.3 Test environment

The experimental frame and test plate were originally assembled at room temperature, about 23°C, for each test item. And all the tests were firstly carried out in this condition as reference. The specimen could be assumed to be stress free without thermal influence at the beginning. During the tests, the plate temperature was elevated step by step. Tests were carried out with temperature increment of about 20°C in the

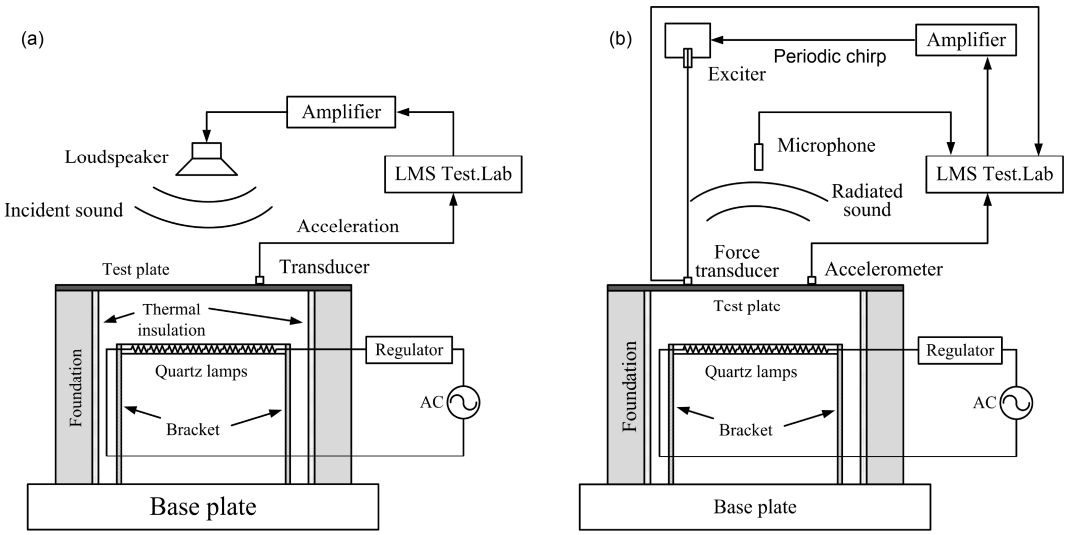

Figure 1 Schematic of the test setup. (a) Acoustic excitation test; (b) mechanical excitation test.

whole temperature range. And denser test points were employed in some temperature range. The maximum test temperature in this work was about 163°C. The plate temperature was measured by thermocouples with an instrumental error of about ±1°C. All the tests were operated in a semi-anechoic environment.

Preliminary tests were conducted to check the uniformity of temperature distribution on the plate. Temperature values on the 36 test points and on the plate edges were compared for each heating condition. The results stated that the maximum temperature discrepancy between the plate center and the edges was generally no more than 20% for the test at 163°C, and the value dropped with the decrement of the plate temperature. To reduce this difference, thermal insulation materials were placed between the specimen and the test frame. The uniformity of temperature distribution was improved to a certain degree. However, the boundary condition was changed greatly. On one hand, the insulation materials were much more flexible than metal. The clamped boundaries, none translations and rotations, could not be achieved by using insulations. On the other hand, the in-plane thermal expansion of the heated plate was released greatly as the insulations could not provide enough compression and friction on plate edges. The static and dynamic characters of the specimen were dramatically changed by these drawbacks. Therefore, insulation materials were finally abandoned. In this paper, the temperature value on the plate center was used to describe the test thermal condition.

3 Experimental results

3.1 Natural vibration

Figure 2 gives the loci of natural frequencies versus temperature measured from modal tests. The results indicate that the whole variation process of natural frequencies can generally be divided into two stages, the descending stage and the ascending stage. In the first stage, all the frequencies decrease as the temperature rises. It shows same variation tendency with the experimental results reported in ref. [27]. In the second stage, frequencies turn to increase.

The fundamental frequency keeps dropping with the increment of plate temperature below about 70°C at which the minimum value appears around 243.2 Hz. Above that temperature, the frequency begins to increase, and finally becomes higher than the initial value, about 454.9 Hz. For mode (2, 1), the minimum value of frequency appears at a higher plate temperature than mode (1, 1). And then, it increases as well. It is clear that the discrepancy between the first and second frequencies is much smaller in the ascending stage.

For modes (1, 2) and (3, 1), the order of the modes interchanges for the first time in their descending stages. This phenomenon was also observed in the previous work [27]. In the ascending stage, mode shape interchange happens again. The order of the two modes regains. For higher order frequencies, ascending stage is not quite clear for some modes in the test temperature range. Mode shape interchange is more common among the frequencies due to higher mode density.

It is obvious that the fundamental frequency is much more sensitive to the temperature change than others. The reduction ratio is also much higher than other frequencies while the minimum value appears. The fundamental frequency drops by almost 50% at about 70°C (T_{I} in Figure 2(a)) from its initial value, and rises to more than 1.4 times of the original value at about 163°C. The maximum reduction ratio for the frequency of mode (2, 1) is about 40% at about 75°C (T_{II} in Figure 2(a)). For higher modes, the reduction ratios are no more than 25% in the test temperature range. And the value drops with the increment of mode order.

For the heated plate, there are two major factors affecting the natural vibrations, thermal stresses and thermal deflection. During heating period, compressive forces generate in the constrained plate, and the values increase with the increment of temperature. As reported in the previous studies [9–14], compressive thermal forces will reduce the stiffness of the plate, natural frequencies decrease under thermal loads. In the meanwhile, the clamped plate deflects in the

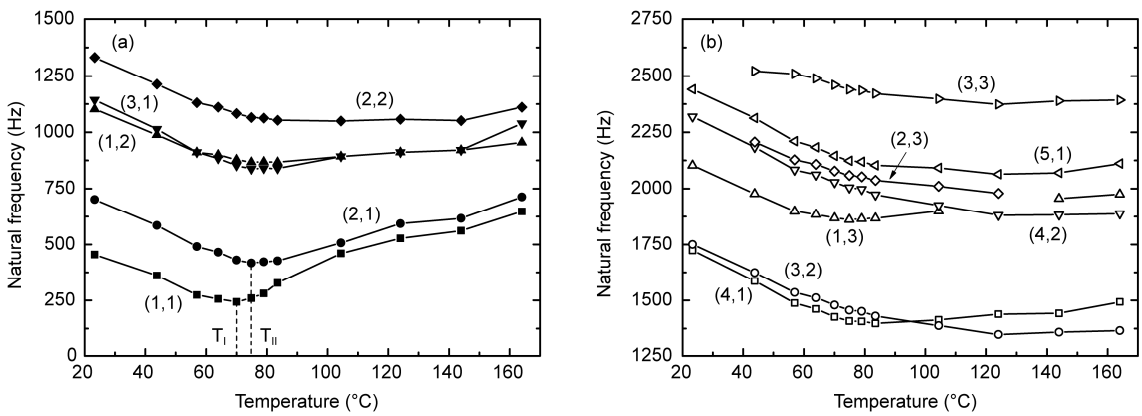

Figure 2 Measured frequency loci. (a) First five modes; (b) higher order modes.

process of heating, and the central deflection of the equilibrium position of the test plate gets larger as the temperature rises. This variation in static configuration provides additional stiffness to the structure compared with flat configuration. It makes the vibrating plate stiffer, and leads to the increment of frequencies. These two factors affect the natural vibration with opposite effects.

As measured from the test, shown in Figure 3, the central deflection of the test plate increases gradually as the temperature is elevated. The variation in thermal deflection of the plate is not obvious below about 43°C, which is slightly lower than the theoretical critical buckling temperature of the plate 49.2°C [12]. Above 43°C, the measured deflection changes suddenly, and the variation ratio jumps as well. The plate buckled due to the thermal load in that temperature range. The continued decrement of the fundamental frequency below about 70°C indicates that the softening effect of thermal stresses plays the crucial role in this temperature range. However, the decrement of reduction speed of fundamental frequency implies that the stiffening effect of the thermal deflection is getting stronger. When the softening effect and the stiffening effect come to an equilibrium point, the frequency achieves the non-zero lowest point. Meanwhile, the current temperature is higher than the theoretical critical buckling temperature. These are caused by the presence of the thermal deflection throughout the test. In the temperature range above 70°C, the thermal buckling deflection of the plate becomes more obvious, and can be observed easily, as displayed in Figure 4. In this stage, both the thermally softening effect and the stiffening effect are getting stronger continuously. And the stiffening effect of the buckling deflection turns to be the leading role. It makes the effective stiffness of the thermal buckled plate increase, and fundamental frequency turns to increase.

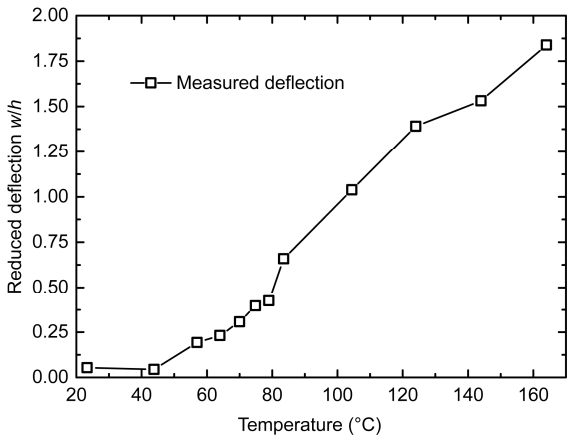

Figure 3 Measured center deflection variation of the test plate.

3.2 Acoustic excitation

The measured vibration responses of the plate, on one of the observation points, under acoustic excitations are given in Figure 5. According to the modal test results, the whole temperature range is here divided into two heating stages by 70°C, at which the minimum value of fundamental frequency appears.

The results demonstrate that the response curve shifts toward the lower frequency range with the increment of temperature in the first heating stage (Figure 5(a)). The global characters of acceleration response almost stay the same. In this temperature range, natural frequencies of the heated plate decrease continuously. It leads to the variation of forced vibration responses. At the first resonant peak, a reduction of the response amplitude can be observed obviously. These variation trends agree with the test results reported in ref. [27] and thermal load softens the clamped plate obviously.

In the second heating stage, the vibration response curve tends to be concentrated in the mid-frequency range from both lower and higher frequency ranges (Figure 5(b)). In this stage, natural frequencies of lower order modes turn to increase successively, while the frequencies of higher order modes still keep dropping. It makes the resonant peaks close up in the mid-frequency range around 750 Hz. The frequency intervals between resonant peaks become smaller, and more peaks appear in the frequency range below 3000 Hz. Different from the responses in stage 1, the global response character is changing as temperature rises. Especially for the test at 163°C, the measured response has already

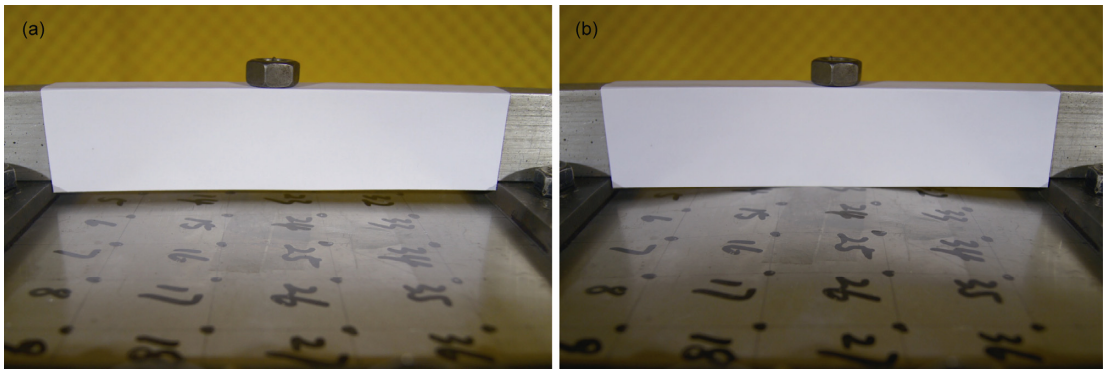

Figure 4 (Color online) Observed deflection of the test plate. (a) At 23°C; (b) at 163°C.

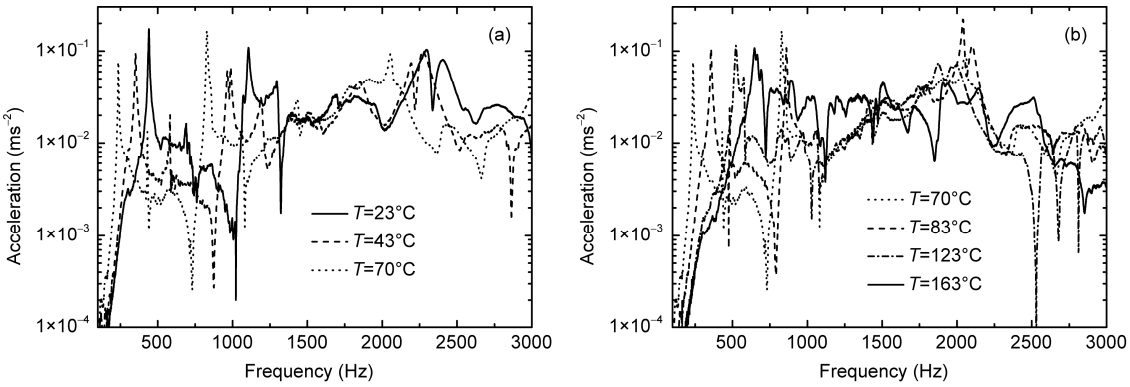

Figure 5 Measured responses under acoustic excitation. (a) Below 70°C; (b) above 70°C.

turned to be another one. Variations in the acceleration responses on other observation points are quite similar. For the post-buckled plate, thermal load stiffens the plate at a certain degree with the buckling deformation. In the meanwhile, the response characters are changed due to the variation in static state of the buckled plate in thermal environments.

3.3 Mechanical excitation

The measured vibration frequency response functions (FRFs) under mechanical excitations in the two heating stages are plotted in Figure 6. In the tests, most of the modes are excited below 3000 Hz, the response are quite complicated in the whole frequency band. Hence datum points above 1500 Hz are left out here. Similar to the acoustic excitation tests, vibration response curve shifts toward the lower frequency range in the first heating stage, and closes up in the mid-frequency range in the second heating stage. The response amplitude of the first resonant peak shows the same variation trend with the results obtained in the acoustic tests in stage 1, and states an opposite trend in stage 2. For the test case of 163°C, the response curve appears like a quite different one. The first resonant amplitude decreases obviously, and shape of the response curve around that frequency changes greatly. This variation was confirmed by tests at the same temperature level repeatedly.

Figure 7 displays the measured sound pressure level (SPL) FRFs at the observation point. As determined by the plate vibration directly, the acoustic radiation responses show the same variation tendency with the acceleration responses, and the first resonant amplitude varies generally in accordance with the amplitude of acceleration, decreases continuously with the increment of temperature.

4 Numerical simulations

In this section, numerical simulations are carried out to study the test results. In finite element formulation, pre-stressed dynamic response analysis of structures can be conducted with the governing equation as [37]

$$\left(\boldsymbol{K}+\boldsymbol{K}_{\sigma}\right)\{\boldsymbol{U}\}+\boldsymbol{M}\left\{\ddot{\boldsymbol{U}}\right\}=\{\boldsymbol{F}\}, \tag{1}$$

where K is the conventional stiffness matrix, M is the mass matrix, $\{U\}$ is the amplitude vector of nodal degree of freedom (d.o.f.), $\left\{\ddot{\boldsymbol{U}}\right\}$ is the acceleration vector of nodal d.o.f., F is the excitation vector, K_{σ} is the stress stiffness matrix which can be defined for plate model as

$$\boldsymbol{K}_{\sigma}=\sum_{i}\int_{A_i}\boldsymbol{G}^{\mathrm{T}}\begin{bmatrix}N_x & N_{xy}\\ N_{xy} & N_y\end{bmatrix}\boldsymbol{G}\mathrm{d}A, \tag{2}$$

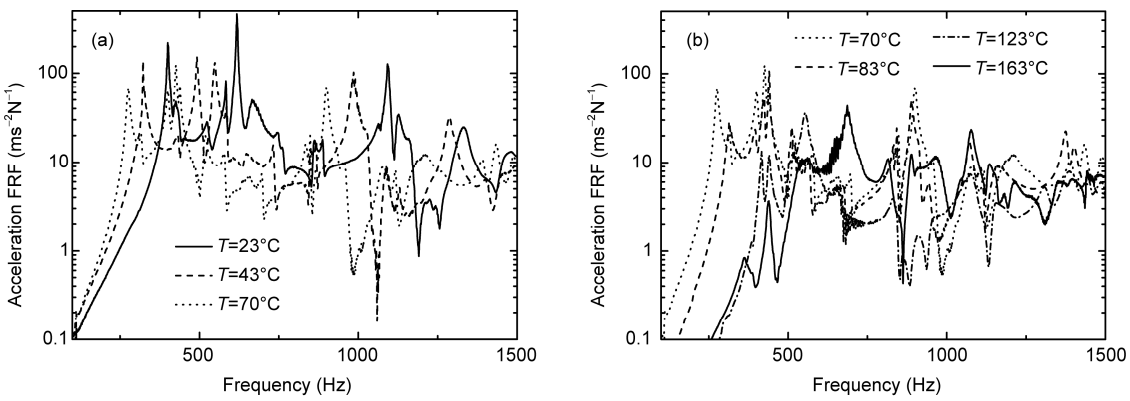

Figure 6 Measured vibration responses under mechanical excitation. (a) Below 70°C; (b) above 70°C.

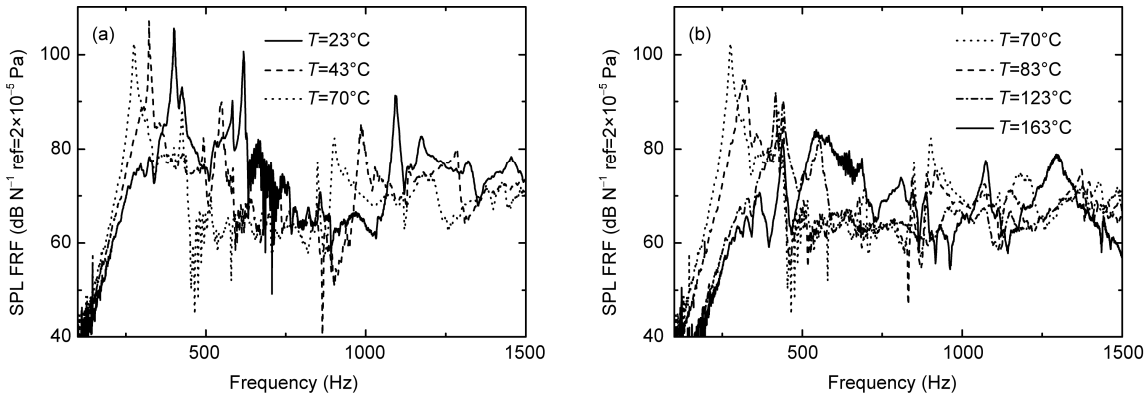

Figure 7 Measured acoustic radiation from the test plate. (a) Below 70°C; (b) above 70°C.

where N_x, N_y, and N_{xy} are the static membrane forces, G is the strain-displacement matrix, A_i is the area of the ith element.

In this work, the pre-stresses are induced by plate temperature variation, and can be obtained by static thermo-elastic analysis firstly. And then, dynamic responses of the heated plates could be predicted via pre-stressed dynamic analysis.

4.1 Modal results

The software package MD NASTRAN was used to perform normal modes analyses. The plate was modeled by 2400 quadrilateral plate elements (CQUAD4) with 60 elements along the length and 40 elements along the width, respectively.

At first, buckling analysis was conducted for the flat plate model with solver sol 105 to determine the critical buckling temperature. As calculated, the critical value is about 49.1°C with the reference temperature of 23°C. It indicates that the clamped plate will lose stability when the temperature is higher than that critical value. Therefore, different computational processes should be selected in calculations for different temperature ranges.

For cases below 49.1°C, linear static solver (sol 101) was used to conduct thermo-elastic analyses first. And then normal mode calculations were carried out with the solver sol 103 by using the thermal stresses as pre-stresses. For cases above 49.1°C, nonlinear solver (sol 106) was used to obtain the thermal stresses and thermal deflections, and predict the natural vibrations of the thermal loaded plate as well.

As shown in Figure 2, all the minimum values of the measured frequencies are non-zero. It means that the test plate does not show the buckling point clearly. This is generally caused by the initial deflection which is inherent for any real structure at room temperature [28]. In finite element simulations for initially curved plates, the geometric imperfection could be considered by modifying the configuration of the plate model. The initial deflections on the 36 test points of the test plate were measured referred to the plate edges, and the results were used to modify the transverse coordinate values of the FE plate model. Therefore, an initially curved plate model could be obtained approximate to the specimen.

Besides the initial deflection, thermal expansion of the experimental frame is another influence factor affecting the dynamic characters of the heated plate. The temperature variation of the test frame is generally inevitable in experiments for hot structures. Thermal expansion of the frame will change the boundary condition of the specimen, and affect the test result in a certain degree. In finite element simulations, the deformation of the frame can be simulated by applying forced displacements on edges. The boundary expansion of the test plate is supposed to be determined by the deformation of the experimental frame, as the frame is stiffer than the specimen. The amounts of the thermal deformation are estimated by multiplying the measured temperature variations of the experimental frame, Young's modulus of steel 200 GPa, Poisson's ratio of steel 0.3, and the original length of the frame. The values are applied on both the longer and the shorter edges of the plate model as forced displacements in static thermo-elastic analyses. Mode analyses of the initially curved plate models were carried out with nonlinear solver sol 106 at every temperature point.

Figure 8 gives the comparisons between the measured natural frequencies and numerical predictions with and without considering the initial curvature (IC) of specimen and the thermal expansion (TE) of frames. For ideal flat plate model, natural frequencies drop to zero in sequence from low order to high order modes with the increment of temperature. It means that the sum of the conventional stiffness and stress stiffness in eq. (1) goes to zero at the critical points.

Compared with the ideal flat plate, the initially curved plate behaves more similarly to the specimen in thermal environments. All the calculated frequencies decrease to non-zero minimum values and turn to increase. The variation tendency is consistent with the measured results. It implies that the softening effect of thermal stresses cannot reduce the natural frequencies to zero due to the existence

of initial deflection, which provides additional stiffness to the structure relative to the flat configuration.

In this condition, the whole stiffness of structures can be decomposed into three parts further: The conventional stiffness referring to flat model, the additional stiffness referring to static curvature, and the stress stiffness referring to thermal stresses. The dynamic function of the heated plate can be expressed as

$$\left(\left(\boldsymbol{K}_f+\boldsymbol{K}_c\right)+\boldsymbol{K}_\sigma\right)\{\boldsymbol{U}\}+\boldsymbol{M}\{\ddot{\boldsymbol{U}}\}=\{\boldsymbol{F}\}, \tag{3}$$

where $\boldsymbol{K}_f$ is the stiffness of the flat plate configuration, $\boldsymbol{K}_c$ is the stiffness caused by curvature including the initial curvature and thermal deformation. In the finite element simulations used here, the stiffness term K in eq. (1) is actually the combination of $\boldsymbol{K}_f$ and $\boldsymbol{K}_c$. For ideal flat plates, $\boldsymbol{K}_c$ does not exist until thermal buckling occurs. For real structures with initial curvature, $\boldsymbol{K}_c$ always exists, and the amount will increase as temperature rises due to thermal deflection. It acts as an inhibiting effect against the softening effect of thermal stresses. At the critical point, the two opposite effects achieve an equilibrium state in which the bending stiffness of the plate is reduced to the minimum value. Accordingly, the frequency drops to the minimum value. Due to the balance of these two effects in thermal environments, the frequency loci behave like upward parabolas.

Analytical results suggest that the critical buckling temperature is determined by geometric parameters and material properties of plates [11]. Being affected by thermal stresses, the bending stiffness of the heated flat plate drops to zero at the critical buckling temperature which can be regarded as the temperature equilibrium point. With considering the initial curvature, the equilibrium state of the plate appears at the temperature lower than the critical buckling value, shown as the dash lines in Figure 8. It indicates that the stiffening effect induced by thermal deflection drives the equilibrium point to move towards lower temperature range. For the cases which take the variation in configuration into account only, it could be imagined that natural frequencies of the heated plate will rise consistently in the whole temperature range, since the thermal deflection enlarges continuously with the increment of temperature. In this condition, frequency loci increase monotonically. It means that the temperature equilibrium point does not exist, or the equilibrium point is driven to lower temperature range and disappears at room temperature which contains on thermal influence. This case can be regarded as a special case considering the influence of temperature variations.

As depicted in Figure 8, frequency loci are much closer to the test ones with considering both the initial deflection of the specimen and the deformation of the frame. The thermal expansion of the frame will release part of the thermal stresses and thermal deflection of the test plate, and both the thermal softening and stiffening effects are reduced accordingly. In the first heating stage, in which the softening effect is dominant, the measured frequencies are higher than the values of plates with idealized boundaries. And in the second heating stage, in which the stiffening effect is dominant, the measured frequencies are lower.

4.2 Dynamic responses

The combined FEM/BEM solver of the software package VA ONE was employed to predict the dynamic response of the plate under excitations. FE plate model with initial curvature, used in modal analyses, was established in VA ONE with NASTRAN input file. Modal parameters were read from the NASTRAN result file with considering both the initial curvature of the specimen and the thermal expansion of the frame for each temperature case. The material damping of the plate was modeled with a constant damping loss factor valued 0.5%, which is assumed to be constant in the frequency bandwidth and in the temperature range. The acoustic medium was modeled with BEM fluid connected to the plate, with speed of sound 343 m s^{-1} and density 1.21 kg m^{-3}.

In acoustic excitation simulations, the acoustic source was applied via monopole source 0.3 m above the FE plate model in the BEM fluid, and the pressure spectrum was

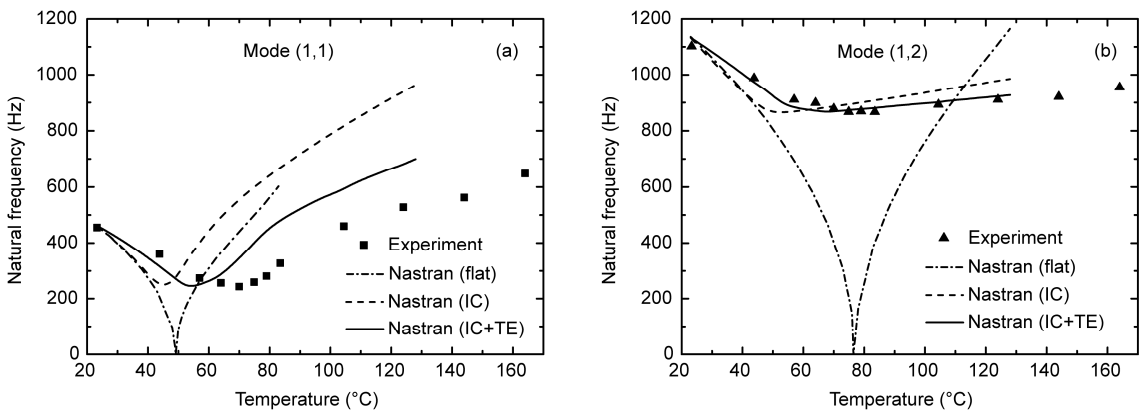

Figure 8 Comparisons between the measured frequencies and the numerical ones considering initial deflection and imperfect boundaries. (a) Mode (1, 1); (b) mode (1, 2).

measured in the tests. In the experiments, it was impossible to set the loudspeaker perfectly on the center line of the plate so an offset value of 3 mm was set to the monopole on both the two perpendicular in-plane directions.

Figure 9 displays the comparisons of acceleration responses between the measured (in Figure 5) and numerical results on the observation point. Three typical thermal conditions in the tests are selected, with temperature states of room temperature, 70, and 123°C, respectively. It can be seen that the simulation result coincides with the test one well at room temperature. For the case at 70°C, the measured fundamental frequency drops to the minimum value, while the calculated frequency had already turned to rise. The prediction error makes the mismatch at the first resonant peak more obvious. For case at 123°C in the post-buckling range, the variation trends of the measured and the calculated fundamental frequencies are the same. Therefore, the first resonant peaks vary synchronously, and the mismatch does not enlarge. In higher frequency range, the measured response peaks appear to be fuzzier than the calculated results. From the above, numerical results reflect the general response variation trend of the experimental results in thermal environments, even if the mismatch of the first resonant peak gets larger due to the prediction error of the fundamental frequency.

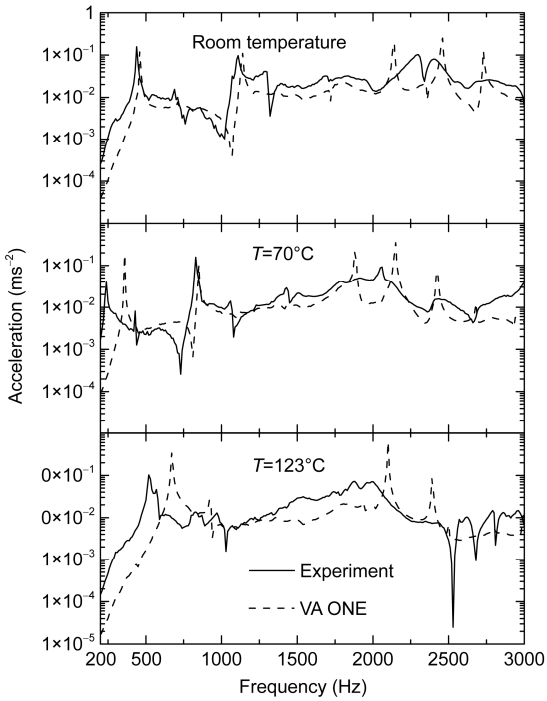

Figure 9 Comparisons between the measured and predicted acceleration responses under acoustic excitation.

In mechanical excitation simulations, the force spectrum of the excitation was set with unit value in the whole frequency range. Figure 10 shows the comparisons of acceleration and SPL responses between the measured (in Figures 6 and 7) and numerical results. It is clear that the shapes of the response curves generally agree, but the response levels and resonant peaks do not match well. It is mainly caused by the presence of the exciter, which changes the mass and the stiffness of the plate with uncertain volumes in thermal tests. In simulations, the mechanical excitation is modeled as an ideal point excitation which has no influence on the inherent characters of structures. The predicted response levels get close to the measured ones as temperature rises. It indicates that the simulated state approaches the actual

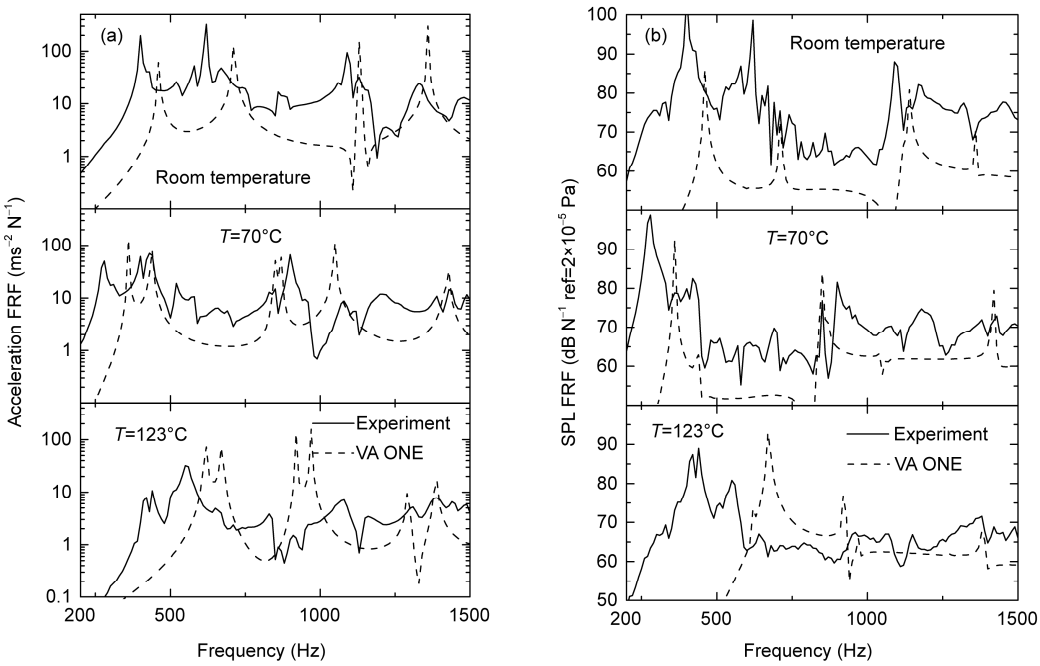

Figure 10 Comparisons between the measured and predicted responses under mechanical excitation: (a) Acceleration FRFs; (b) SPL FRFs.

environment, although the mismatch still exists. Even so, the numerical results still give the general variation trend of the measured results.

5 Conclusions

Experiments were carried out for the heated plate in both pre- and post-buckling ranges in this work. Modal tests and dynamic response tests were performed in temperature range below and above the theoretical critical buckling temperature of the plate. Modal results indicate that natural frequencies of the heated clamped plate show a decrement-increment variation trend as temperature rises. The softening effect of thermal stresses plays the leading role before buckling, and the stiffening effect of thermal deflection becomes the key influence factor for the thermal post-buckled plate. Numerical simulations showed that natural frequencies of the plate will not drop to zero in thermal environments because of the inherent initial deflection. The stiffening effect of thermal deflection drives the equilibrium temperature point to move towards lower temperature range.

Dynamic response and acoustic radiation response of the heated plate show two variation trends in the whole temperature range. In the first heating stage, response curves shift toward the lower frequency range, the global response character almost stays the same. In the second stage, response curves close up in the mid-frequency range and the shape of responses changes gradually. Thermal load stiffens the buckled plate in a certain degree, but changes the response characters of the heated plate. The variation trend of responses becomes more complicated in thermal environments.

This work was supported by the National Natural Science Foundation of China (Grant Nos. 11321062, 11472206 and 91016008).

1 Behrens B, Muller M. Technologies for thermal protection systems applied on re-usable launcher. Acta Astronautica, 2004, 55: 529–536
2 Zhao J S, Gu L X, Ma H Z. A rapid approach to convective aero-heating prediction of hypersonic vehicles. Sci China Tech Sci, 2013, 56: 2010–2024
3 Zhu S Y, Zhu L W. Vibration test condition for spacecraft lift-out environment. Sci China Tech Sci, 2012, 55: 1954–1959
4 Li D X, Xu R. Autonomous decentralized intelligent vibration control for large split-blanket solar arrays. Sci China Tech Sci, 2013, 56: 703–712
5 Cui K, Hu S C, Li G L, et al. Conceptual design and aerodynamic evaluation of hypersonic airplane with double flanking air inlets. Sci China Tech Sci, 2013, 56: 1980–1988
6 Sun Q, Cheng B Q, Li Y H, et al. Computational and experimental analysis of Mach 2 air flow over a blunt body with plasma aerodynamic actuation. Sci China Tech Sci, 2013, 56: 795–802
7 Behnek M N, Sharma A, Przekop A, et al. Thermal-acoustic analysis of a metallic integrated thermal protection system structure. In: American Institute of Aeronautics and Astronautics Inc. 51st AIAA/ASME/ASCE/AHS/ASC Structures, Structural Dynamics, and Materials Conference, Orlando, Florida, USA, April 12–15, 2010
8 Yang X W, Wang C, Li Y M, et al. Vibro-acoustic response of a thermally stressed reinforced conical shell. Advanced Sci Lett, 2011, 4: 2802–2806
9 Jeyaraj P, Padmanabhan C, Ganesan N. Vibration and acoustic response of an isotropic plate in a thermal environment. ASME Trans J Vib Acoust, 2008, 130: 70510055
10 Jeyaraj P, Ganesan N, Padmanabhan C. Vibration and acoustic response of a composite plate with inherent material damping in a thermal environment. J Sound Vib, 2009, 320: 322–338
11 Geng Q, Li Y M. Analysis of dynamic and acoustic radiation characters for a flat plate under thermal environments. Int J Appl Mech, 2012, 4: 1250028
12 Geng Q, Li Y M. Solutions of dynamic and acoustic responses of a clamped rectangular plate in thermal environments. J Vib Control, 2014, doi: 10.1177/1077546314543730
13 Liu Y, Li Y M. Vibration and acoustic response of rectangular sandwich plate under thermal environment. Shock Vib, 2013, 20: 1011–1030
14 Li W, Li Y M. Vibration and sound radiation of a laminated rectangular plate in thermal environments. Acta Mechanica Solida Sinica, 2015, 28: 11–22
15 McWithey R R, Vosteen L F. Effects of transient heating on the vibration frequencies of a prototype of the X-15 wing. NASA Technical Note No. 362, 1960
16 Brown A M. Temperature-dependent modal test/analysis correlation of X-34 FASTRAC composite rocket nozzle. J Propulsion Power, 2002, 18: 284–288
17 Hudson L D, Stephens C A. X-37 C/SiC ruddervator subcomponent test program. NASA Technical Report No. DFRC-1069, 2009
18 Natalie D S. High-temperature modal survey of a hot-structure control surface. In: ICAS Secretariat. Proceedings of 27th Congress of International Council of the Aeronautical Sciences, Nice, France, September 19–24, 2010
19 Wu D F, Zhao S G, Pan B, et al. Experimental study on high temperature thermal-vibration characteristics for hollow wing structure of high-speed flight vehicles (in Chinese). Chin J Theo Appl Mech, 2013, 45: 598–605
20 Vosteen L F, Fuller K E. Behavior of a Cantilever Plate under Rapid-heating Conditions. NACA Research Memorandum No. L55E20c, 1955
21 Vosteen L F, McWithey R R, Thomosn R G. Effect of transient heating on vibration frequencies of some simple wing structures. NACA Technical Note No. 4054, 1957
22 Kehoe M W, Snyder H T. Thermoelastic vibration test techniques. NASA Technical Memorandum No. 101742, 1991
23 Snyder H T, Kehoe M W. Determination of the effects of heating on modal characteristics of an aluminum plate with application to hypersonic vehicles. NASA Technical Memorandum No. 4274, 1991
24 Kehoe M W, Deaton V C. Correlation of analytical and experimental hot structure vibration results. NASA Technical Memorandum No. 104269, 1993
25 Amabili M, Carra S. Thermal effects on geometrically nonlinear vibrations of rectangular plates with fixed edges. J Sound Vib, 2009, 321: 936–954
26 Joen B H, Kang H W, Lee Y S. Free vibration characteristics of rectangular plate under rapid thermal loading. In: Trans Tech Publications Ltd. 9th International Congress on Thermal Stress, Budapest, Hungary, June 5–9, 2011
27 Geng Q, Li H, Li Y M. Dynamic and acoustic response of a clamped rectangular plate in thermal environments: Experiment and numerical simulation. J Acoust Soc Am, 2014, 135: 2674–2682
28 Murphy K D, Ferreira D. Thermal buckling of rectangular plates. Int J Solids Structures, 2001, 38: 3979–3994
29 Chu G P, Li Z M. Postbuckling behavior of 3D braided rectangular plates subjected to uniaxial compression and transverse loads in thermal environments. Sci China Tech Sci, 2014, 57: 1439–1453
30 Tawfik M, Ro J J, Mei C. Thermal post-buckling and aeroelastic behaviour of shape memory alloy reinforced plates. Smart Mater Structures, 2002, 11: 297–307
31 Singha M K, Ramachandra L S, Bandyopadhyay J N. Vibration behavior of thermally stressed composite skew plate. J Sound Vib, 2006,

296: 1093–1102
32 Xia X K, Shen H S. Vibration of postbuckled FGM hybrid laminated plates in thermal environment. Eng Structures, 2008, 30: 2420–2435
33 Xia X K, Shen H S. Vibration of post-buckled sandwich plates with FGM face sheets in a thermal environment. J Sound Vib, 2008, 314: 254–274
34 Fazzolari F A, Carrera E. Accurate free vibration analysis of thermo-mechanically pre/post-buckled anisotropic multilayered plates based on a refined hierarchical trigonometric Ritz formulation. Composite Structures, 2013, 95: 381–402
35 Murphy K D, Virgin L N, Rizzi S A. Free Vibration of Thermally Loaded Panels Including Initial Imperfections and Post-buckling Effects. NASA Technical Memorandum No. 109097, 1994
36 Murphy K D, Virgin L N, Rizzi S A. The effect of thermal prestress on the free vibration characteristics of clamped rectangular plates: Theory and experiment. ASME Trans J Vib Acoust, 1997, 119: 243–249
37 Cook R, Malkus D, Plesha M. Concepts and Application of Finite Element Analysis. 3rd eds. New York: Wiley, 1989. 429–446